694. Development of spherical ultrasonic motor for pipe inspection robot

S. Toyama[a], M. Hoshina[b]
Tokyo A&T University, Koganei, Tokyo, Japan
E-mail: [a]*toyama@cc.tuat.ac.j,* [b] *50010643225@st.tuat.ac.jp*
Phone: +81423887207, **Fax:** +81423887207

Abstract. We present a pipe inspection robot using a newly developed spherical ultrasonic motor (SUSM) as a camera actuator. The novel SUSM has improved the range of movement compared to previous SUSMs, and the robot can point a camera in any direction. In this study, we determined a method for controlling the rotational direction and strategic control from the kinematics and characteristics of ultrasonic motors. The rotational directions were defined by the phase differences of the applied voltages, and the rotational speeds were changed with the frequencies. Additionally, we developed a very small position sensing system using rotary potentiometers. In the control experiment performed using the sensing system, the SUSM showed the returnability to the default position from several specified points, within an accuracy of 1°.

Keywords: ultrasonic motor, pipe inspection, PZT, spherical motor.

Introduction

Many research groups have attempted the development of compact pipe inspection robots with new actuation to detect flaws and rust in pipe directories [1–10]. Pipe inspection devices using a camera with fish-eye lens suffer from the disadvantage that small details cannot be observed. Pneumatic actuators [1–3], shaped memory alloys (SMAs) [4], piezoelectric actuators [5, 6], and giant magnetostrictive alloys [7] have been employed to incline the head carrying the camera in the robots. Pneumatic wobble motors, which are compact and flexible actuators, rotate the camera and hands of the robot [8]. Snake robots, which aim to move in a pipe, also have cameras at the head of the robot and they can incline their head [9, 10].

Kinematic Design of Actuator and Sensing System

The SUSM comprises three ring-shaped vibrators and one sphere. The vibrator consists of an annular metallic elastic body to which piezoelectric elements are glued. When an AC voltage is applied to the piezoelectric elements, a standing wave is generated on the elastic body. When two AC voltages with a time phase difference are applied to the positive and negative sections of the piezoelectric elements, a traveling-wave is generated due to combination of the two standing-waves. The vibrators provide vibration energy to the sphere by an elliptical motion generated by the traveling wave. We can control the magnitude and direction of the torque by changing the phase difference.

The relationship between the torque T and phase difference ρ in a single vibrator is approximated by the following equation:

$$T = A\sin\rho \quad (1)$$

where A is the maximum value of the torque. The torque of the SUSM is determined by the resultant vector of the vibrators. Fig. 1 shows the locations of the vibrators and sphere along the *X-Y* and *X-Z* planes, respectively. The components of the resultant vector generated by each vibrator, $\mathbf{S}_1$, $\mathbf{S}_2$ and $\mathbf{S}_3$, are described by the following equations:

$$\mathbf{S}_1 = T_1\left[\cos\frac{3}{2}\pi\cos\phi \quad \sin\frac{3}{2}\pi\cos\phi \quad \sin\phi\right]^T$$
$$\mathbf{S}_2 = T_2\left[\cos\frac{5}{6}\pi\cos\phi \quad \sin\frac{5}{6}\pi\cos\phi \quad \sin\phi\right]^T \tag{2}$$
$$\mathbf{S}_3 = T_3\left[\cos\frac{1}{6}\pi\cos\phi \quad \sin\frac{1}{6}\pi\cos\phi \quad \sin\phi\right]^T$$

where T_1, T_2, and T_3 are the scalars of the torque generated by each vibrator, respectively. ϕ is the angle with the *X*-*Y* plane, as shown in Fig. 1(b). The resultant vector of the torque generated by SUSM, $\mathbf{S}$, is described as follows:

$$\mathbf{S} = \mathbf{S}_1 + \mathbf{S}_2 + \mathbf{S}_3 \tag{3}$$

$$\mathbf{S} = \begin{bmatrix} S_x \\ S_y \\ S_z \end{bmatrix} = \begin{bmatrix} \left(-\frac{\sqrt{3}}{2}T_2 + \frac{\sqrt{3}}{2}T_3\right)\cos\phi \\ \left(-T_1 + \frac{1}{2}T_2 + \frac{1}{2}T_3\right)\cos\phi \\ \left(T_1 + T_2 + T_3\right)\sin\phi \end{bmatrix} \tag{4}$$

Here, the torque of the SUSM has three rotational DOFs. By controlling the torque of each vibrator, the SUSM generates a torque between the outer case and the sphere.

The rotational direction of the SUSM is defined by the differences in the input phase of each vibrator. To avoid rotating camera footage, the rotation around the *Z*-axis is restricted when the SUSM is used as a camera actuator in the pipe inspection robot:

$$S_z = 0 \tag{5}$$

In addition, the scalar of the SUSM torque should be constant in order to equalize the rotational speeds in all rotational directions:

$$|\mathbf{S}| = B \tag{6}$$

Here, B is a constant number. We defined the angle from the Y-axis, ψ, to the rotational vector on the X-Y plane, as shown in Fig. 1(a). The torques of each vibrator, T_1, T_2, and T_3, are described by the following equations, Eqs. (4) – (6), respectively:

$$T_1 = C\cos\psi$$
$$T_2 = C\cos\left(\psi + \frac{2}{3}\pi\right) \tag{7}$$
$$T_3 = C\cos\left(\psi - \frac{2}{3}\pi\right)$$

$$C = \frac{2}{3}\frac{B}{\cos\phi} \tag{8}$$

The torque of the SUSM becomes maximum when the following condition is applied to Eq. (1) and (7):

$$C_{\max} = A \tag{9}$$

Using Eqs. (6), (8), and (9), the maximum torque of the SUSM is described as follows:

$$|\mathbf{S}|_{\max} = \frac{2}{3}\cos\phi \cdot A \tag{10}$$

The maximum torque of the SUSM is approximately 1.5 times larger than that of one vibrator when the angle ϕ is small. When the rotational direction is given, the input phase differences of each vibrator, ρ_1, ρ_2, and ρ_3, are defined by the following equations:

$$\rho_1 = \sin^{-1}(\cos\psi)$$
$$\rho_2 = \sin^{-1}\left(\cos\left(\psi + \frac{2}{3}\pi\right)\right) \quad (11)$$
$$\rho_3 = \sin^{-1}\left(\cos\left(\psi - \frac{2}{3}\pi\right)\right)$$

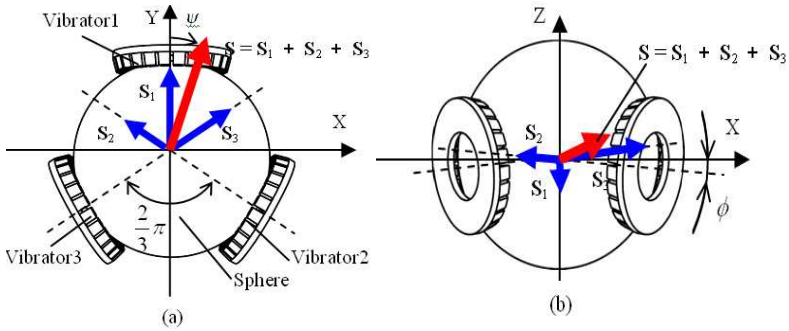

Fig. 1. Location of the vibrators (a) *x-y* plane, (b) *x-z* plane

Experiments of SUSM

The characteristics of the torque and rotational speed and those of the phase difference and rotational speed were measured. Figs. 2-4 demonstrate the schematic of the experimental setup. The equipment comprises an SUSM at the center and two rotary encoders (MES-20-3600P) manufactured by MTL located at right angles to each other. The encoders with circular arch-shaped guides measure the rotational angle of the SUSM.

The relationship between the torque and the rotational speed was measured. The output axis was an added weight with a thread. The amount of weight was varied, and the rotational speed was measured. The rotational speed was measured with a steady speed in order to avoid the effect of the acceleration of the weight. This experiment was conducted with both conventional SUSMs and OR-SUSMs. Fig. 5 shows the results of the characteristics of the torque and rotational speed, indicating that it is linear. There is little difference between the conventional and outer rotor types. The new case has satisfactorily prevented the loss of torque.

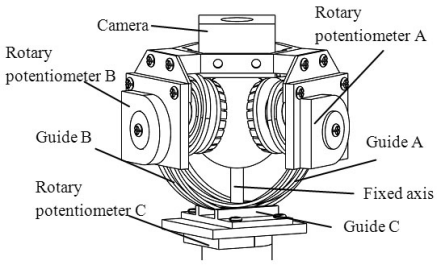

Fig. 2. Position sensing system using rotary potentiometers

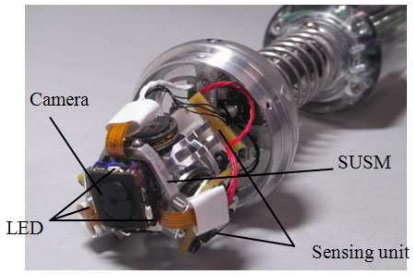

Fig. 3. Head unit of pipe inspection robot with a camera unit in the head of the robot

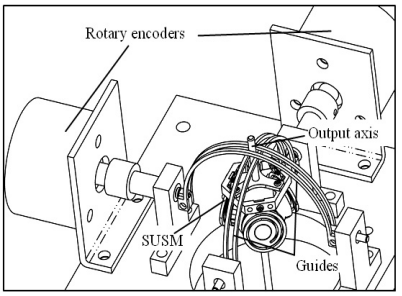

Fig. 4. Schematic of the experimental setup for measuring angle

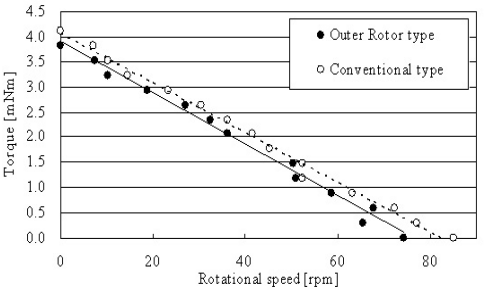

Fig. 5. Relationship between torque and rotational speed

Conclusions

In this study, we developed a novel SUSM (outer rotor-type SUSM) as the camera actuator for a pipe inspection robot. The OR-SUSM dramatically succeeded in expanding the range of movement from 60° to 270°, and decreasing the weight of the case for the OR-SUSM. An FEM analysis and an experiment to evaluate the OR-SUSM were conducted.

We have presented a hybrid control strategy using the phase differences and frequencies of applied voltages to move to designated directions. A compact position sensing system using rotary potentiometers was developed. The total size of the pipe inspection robot can be inserted into the interior of a 50-mm inner diameter pipe. By using this sensing system, the SUSM can return to the default position within accuracy of 1°.

References

[1] Fukuda T., Hosokai H., Uemura M. Rubber gas actuator driven by hydrogen storage alloy for in-pipe inspection mobile robot with flexible structure. ICRA, 1989, p. 1847-1852.

[2] Anthierens C., Ciftci A., Betemps M. Design of an electro pneumatic micro robot for in-pipe inspection. ISIE, 1999, 2, p. 968-972.

[3] Chang-Hwan C., Seung-Ho J., Seung-Ho K. Feeder Pipe Inspection Robot Using an Inch-Worm Mechanism with Pneumatic Actuators. ROBIO, 2004, p. 889-894.

[4] Brunete A., Hernando M., Gambao E. Modular Multiconfigurable Architecture for Low Diameter Pipe Inspection Microrobots. ICRA, 2005, p. 490-495.

[5] Matsuoka T., Okamoto H., Asano M., Mitsuishi S., Matsui T. A prototype model of micro mobile machine with piezoelectric driving force actuator. Proceedings of 5th International Symposium on Micro Machine and Human Science, 1994, p. 47-52.

[6] Idogaki T., Kanayama H., Ohya N., Suzuki H., Hattori T. Characteristics of piezoelectric locomotive mechanism for an in-pipe micro inspection machine. MHS, 1995, p. 193-198.

[7] Fukuda T., Hosokai H., Ohyama H., Hashimoto H., Arai F. Giant magnetostrictive alloy (GMA) applications to micro mobile robot as a micro actuator without power supply cables. MEMS, 1991, p. 210-215.

[8] Suzumori K., Miyagawa T., Kimura M., Hasegawa Y. Micro inspection robot for 1-in pipes. IEEE/ASME Transactions on Mechatronics, 1999, 4(3), p. 286-292.

[9] Hirose S. Biologically Inspired Robots: Snake-Like Locomotors and Manipulators: Oxford University Press, 1993.

[10] Wakimoto S., Nakajima J., Takata M., Kanda T., Suzumori K. A micro snake-like robot for small pipe inspection. MHS, 2003, p. 303-308.